The human LSm1-7 proteins colocalize with the mRNA-degrading enzymes Dcp1/2 and Xrnl in distinct cytoplasmic foci

D. Ingelfinger, D. J. Arndt-Jovin, R. Luhrmann and T. Achsel

RNA 2002 8: 1489-1501

RNA (2002), *8*:1489–1501. Cambridge University Press. Printed in the USA.

DOI: 10.1017/S1355838202021726

The human LSm1-7 proteins colocalize with the mRNA-degrading enzymes Dcp1/2 and Xrn1 in distinct cytoplasmic foci

DIERK INGELFINGER,[1] DONNA J. ARNDT-JOVIN,[2] REINHARD LÜHRMANN,[1] and TILMANN ACHSEL[1,3]

[1]Department of Cellular Biochemistry, Max Planck Institute for Biophysical Chemistry, Am Faßberg 11, 37077 Göttingen, Germany
[2]Department of Molecular Biology, Max Planck Institute for Biophysical Chemistry, Am Faßberg 11, 37077 Göttingen, Germany

ABSTRACT

Sm and Sm-like (LSm) proteins form heptameric complexes that are involved in various steps of RNA metabolism. In yeast, the Lsm1–7 complex functions in mRNA degradation and is associated with several enzymes of this pathway, while the complex LSm2–8, the composition of which largely overlaps with that of LSm1–7, has a role in pre-mRNA splicing. A human gene encoding an LSm1 homolog has been identified, but its role in mRNA degradation has yet to be elucidated. We performed subcellular localization studies and found hLSm1 predominantly in the cytoplasm. However, it is not distributed evenly; rather, it is highly enriched in small, discrete foci. The endogenous hLSm4 is similarly localized, as are the overexpressed proteins hLSm1–7, but not hLSm8. The foci also contain two key factors in mRNA degradation, namely the decapping enzyme hDcp1/2 and the exonuclease hXrn1. Moreover, coexpression of wild-type and mutant LSm proteins, as well as fluorescence resonance energy transfer (FRET) studies, indicate that the mammalian proteins hLSm1–7 form a complex similar to the one found in yeast, and that complex formation is required for enrichment of the proteins in the cytoplasmic foci. Therefore, the foci contain a partially or fully assembled machinery for the degradation of mRNA.

Keywords: exoribonucleases; messenger RNA; ribonucleoproteins; RNA caps

INTRODUCTION

Complete regulation of gene expression can only be achieved if the mRNAs are degraded after a given time, or in response to a regulatory signal. In the yeast *Saccharomyces cerevisiae*, cytoplasmic mRNA degradation is a highly ordered process. It is initiated by the detection of a premature stop codon [nonsense-mediated decay (NMD)], or by the loss of the poly(A) tail, which can occur either by successive deadenylation or by an endonucleolytic cut in the 3′ untranslated region (Hentze & Kulozik, 1999; Tucker & Parker, 2000). As the first step of the actual mRNA decay, the decapping enzyme (which consists of the two subunits Dcp1p and Dcp2p) removes the cap structure from the 5′ end of the mRNA. Then, the exonuclease Xrn1p degrades the mRNA from the 5′ to the 3′ end. A 3′-to-5′ decay is also observed, but it does not contribute significantly to mRNA degradation as long the as 5′-to-3′ pathway can operate (Mitchell & Tollervey, 2000). Recently, it was observed that several Sm-like proteins (Lsm1p to Lsm7p) are required for the 5′-to-3′ mRNA decay (Boeck et al., 1998; Bouveret et al., 2000; Tharun et al., 2000). These proteins associate with the mRNA after deadenylation and recruit at least the decapping enzyme to the mRNA (Tharun & Parker, 2001). In particular, it has been shown that the Lsm proteins form a stable complex with the decapping enzyme Dcp1p (Tharun et al., 2000) and the exonuclease Xrn1p (Bouveret et al., 2000), thus forming a decay machine.

The presence of Sm-like proteins in the mRNA decay machinery is particularly remarkable because Sm and Sm-like proteins have so far only been found associated with small nuclear RNP particles. The family of Sm and Sm-like proteins is defined by the presence of a common, bipartite sequence motif that consists of seven highly conserved amino acids embedded in a

[3]Present address: Fondazione Santa Lucia, Via Ardeatina 354, 00179 Rome, Italy.

Reprint requests to: Dr. Tilmann Achsel, Fondazione Santa Lucia, Via Ardeatina 354, 00179 Rome, Italy; e-mail: tachsel@gwdg.de; or Dr. Reinhard Lührmann, Max Planck Institute for Biophysical Chemistry, Am Faßberg 11, 37077 Göttingen, Germany; e-mail: reinhard.lührmann@mpi-bpc.mpg.de.

characteristic pattern of hydrophobic and hydrophilic amino acids (Hermann et al., 1995; Séraphin, 1995). All family members that have been thoroughly characterized at the biochemical level oligomerize to form a ring-shaped heptamer that binds to RNA with a preference for oligo[U] (Kambach et al., 1999, and references therein; Achsel et al., 1999, 2001). The Sm domain is necessary and sufficient both for Sm protein oligomerization and for specific RNA binding. Three sets of Sm/LSm proteins are associated with snRNPs. First, there are the Sm proteins proper; these form the core of the spliceosomal snRNPs U1, U2, U4, and U5. The Sm core RNPs assemble in the cytoplasm into the heteromers SmB-D3, SmD1-D2, and SmE-F-G; these then bind in an ordered manner onto the U-rich Sm site found in the respective snRNAs. In vivo, Sm assembly occurs in the cytoplasm and requires a complex centered on the survival of motor neurons (SMN) protein (Fischer et al., 1997; Liu et al., 1997). The SMN complex primarily recognizes an unusual posttranslational modification in the RG-rich C-termini found in SmD1 and D3 (Brahms et al., 2000, 2001; Friesen et al., 2001). The Sm core plays a pivotal role in virtually all aspects of the life cycle of the respective snRNPs, including their biogenesis, stability, nuclear import, and subnuclear localization. Secondly, the U7 snRNP involved in histone mRNA processing has an Sm core that contains all Sm proteins except D1 and D2. Instead, it contains at least one Sm-like protein, LSm10 (Pillai et al., 2001). Finally, the LSm2–8 proteins bind to U6 snRNA (Mayes et al., 1999; Salgado-Garrido et al., 1999) at its 3′-terminal oligo[U] stretch (Achsel et al., 1999; Vidal et al., 1999). Like the Sm proteins, the LSm2–8 complex is required for stability of its RNA (Pannone et al., 1998; Mayes et al., 1999; Salgado-Garrido et al., 1999), and there is also evidence that it is needed for snRNP biogenesis, namely in the assembly of the functional U4/U6 di-snRNP (Achsel et al., 1999). It is noteworthy that this nuclear complex contains six out of seven proteins in common with the cytoplasmic LSm1–7 complex.

Much less is known about mRNA degradation in higher eukaryotes. In mammals, the decay triggered by AU-rich instability elements seems to be catalyzed predominantly by the exosome, which moves from 3′ to 5′ (Brewer, 1998; Chen et al., 2001; Wang & Kiledjian, 2001). Furthermore, there appears also to be a 5′-to-3′ degradation pathway, because the 5′ exonuclease Xrn1p (Bashkirov et al., 1997) and the decapping enzyme Dcp1p/Dcp2p (J. Lykke-Andersen, 2002) each have a homolog in mammals. However, it remains an open question whether these activities are also concentrated in a larger complex comparable to the one found in yeast. In particular, it is unclear whether the Sm-like proteins have a role in mammalian mRNA degradation. In this work, we have characterized the apparent human homolog of the yeast LSm1p protein. Interestingly, we find that it is highly enriched, together with the proteins hLSm2–7, in novel foci found in the cytoplasm of human HeLa cells; moreover, several lines of evidence suggest strongly that these foci contain assembled, functional LSm1–7 heptamers. In addition, both the decapping enzyme hDcp1/hDcp2 and the exonuclease hXrn1 are also enriched in these foci. Thus, our results indicate that hLSm1 forms an hLSm1–7 complex in human cells as well, and that this complex is linked to mRNA degradation. Furthermore, important parts of the mRNA degradation machine that have been described for yeast are found highly enriched in foci dispersed throughout the cytoplasm of the human cell. Whether these cytoplasmic foci act as actual degradation centers, as assembly points, or as storage sites remains to be seen.

RESULTS

The human proteins LSm1–7, but not LSm8, accumulate in cytoplasmic foci

To obtain a first hint about the function of the human protein LSm1, we studied its subcellular distribution. Antibodies were raised against a peptide derived from the C terminus of hLSm1, affinity-purified from the serum, and coupled to the fluorescent dye Alexa488 (see Materials and Methods). These antibodies were used to stain human HeLa cells, and images were obtained by confocal microscopy. As shown in Figure 1A, hLSm1 was found almost exclusively in the cytoplasmic compartment, suggesting that hLSm1 has a cytoplasmic function. Strikingly, however, the protein was not evenly distributed throughout the cytoplasm, but was highly enriched in small discrete foci. To find out whether other hLSm proteins were also found in these cytoplasmic foci, we counterstained with hLSm4 antibodies (Achsel et al., 1999) that were likewise affinity-purified and labeled with the Cy3 dye. Significantly, the hLSm4 antibodies also marked cytoplasmic foci (Fig. 1B), and the overlay of the two images demonstrated that these foci were indeed identical (Fig. 1C). In addition, hLSm4 was also detected in the nucleus (Fig. 1B), in accordance with its role in pre-mRNA splicing (see Introduction). Unlike other splicing factors, however, hLSm4 was distributed relatively uniformly in the nucleus, and the nucleoli were also stained to some extent. The nucleolar localization of hLSm4 was confirmed by confocal microscopy counterstaining with anti-fibrillarin antibodies as a nucleolar marker (data not shown). The function of hLSm4 in the nucleolus is not clear. In this respect, it is interesting to note that a complex of LSm proteins that includes LSm4 can bind specifically to the U8 snoRNA (Tomasevic & Peculis, 2002).

Next, it was important to determine whether only the hLSm proteins 1–7, which have a cytoplasmic function in yeast, were enriched in the cytoplasmic foci, or

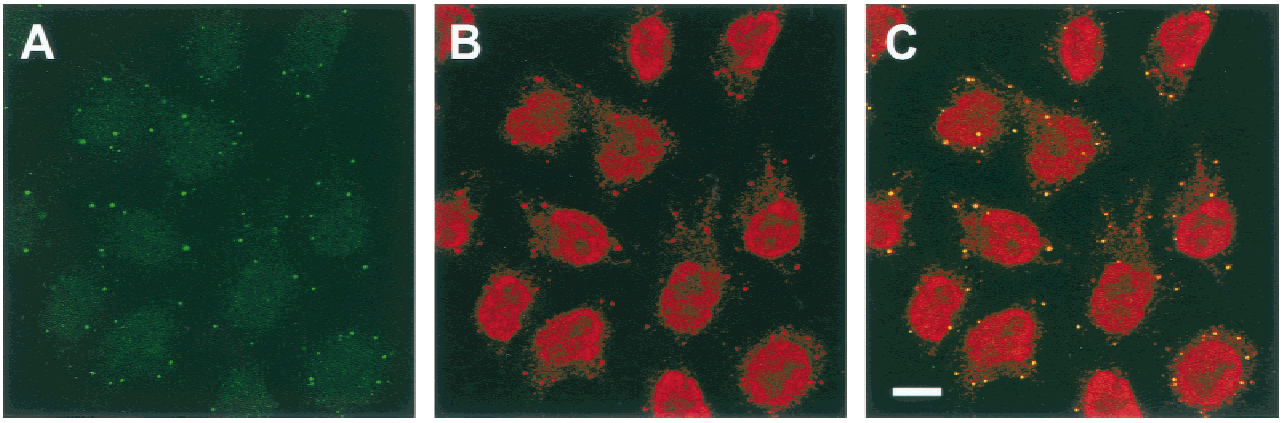

FIGURE 1. Colocalization of the hLSm1 and hLSm4 proteins in cytoplasmic foci. HeLa SS6 cells were grown on cover slips, fixed, stained with Alexa488-conjugated anti-hLSm1 and Cy3-conjugated anti-hLSm4 antibodies, and visualized by confocal microscopy. The panels show a single section, with green representing anti-hLSm1 (**A**, **C**), and red anti-hLSm4 (**B**, **C**). In the overlay picture (**C**), overlap of the colors appears yellow. Scale bar = 10 μm.

whether more hLSm proteins are found there. Because it was not possible to obtain sufficiently specific antibodies against the other hLSm proteins, we transiently expressed YFP-tagged versions of the hLSm proteins in HeLa cells. As shown in Figure 2, the tagged hLSm1 and hLSm4 proteins exhibit localization patterns very similar to that of the endogenous proteins (compare panels A and D with Fig. 1). In addition, the proteins hLSm3, 4, 6, and 7 accumulated in clearly visible cytoplasmic foci. Proteins hLSm5 and, especially, hLSm2 were also detected in the cytoplasm, but these were incorporated less efficiently into foci (Fig. 2B, E; marked by arrowheads). Only YFP-LSm8 was detected almost exclusively in the nucleus and was never observed in cytoplasmic foci (Fig. 2H). Thus, we conclude that all hLSm proteins 1 to 7, but not hLSm8, accumulate in

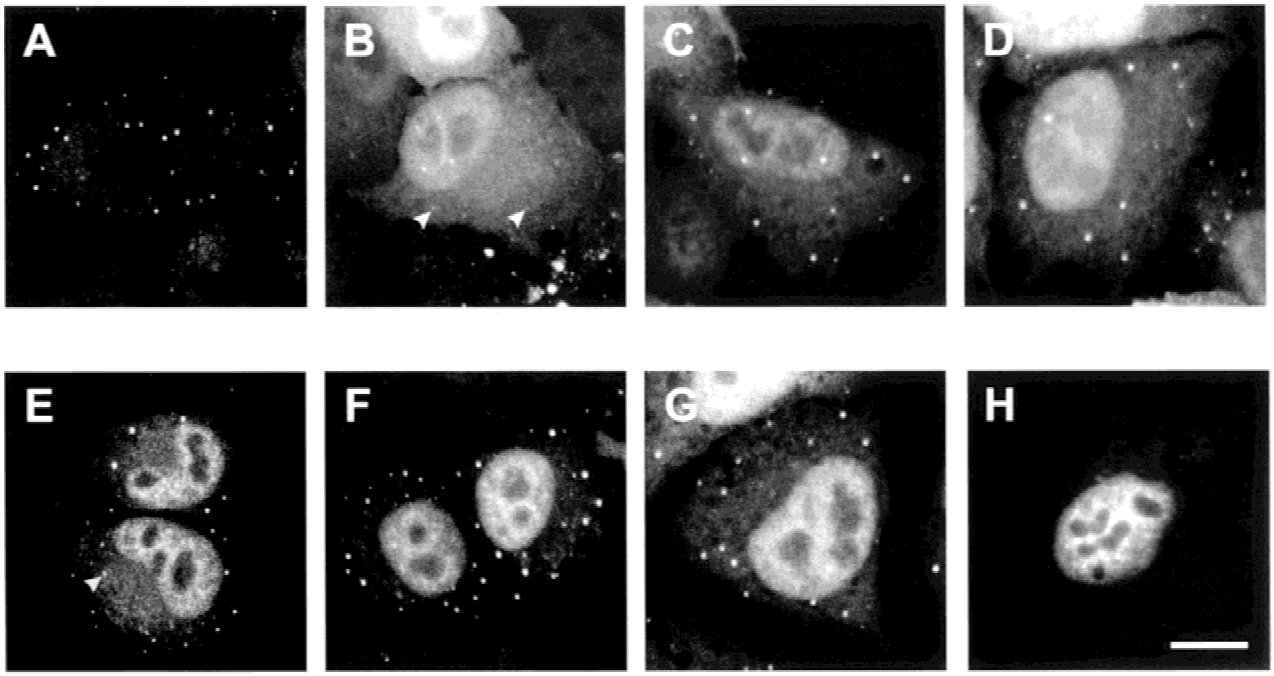

FIGURE 2. Localization of YFP-hLSm1–7, but not YFP-hLSm8, in the cytoplasmic foci. HeLa cells expressing fusion proteins YFP-hLSm1–8 were grown on cover slips, fixed 30 h after transfection, and visualized by confocal microscopy. For each fusion protein, 10 confocal sections were taken. The sections were combined by using the maximum-intensity algorithm of the MetaView imaging software (Version 4.5r5) to obtain a high-quality view of the whole cell. The panels show the following overexpressions: **A:** hLSm1; **B:** hLSm2; **C:** hLSm3; **D:** hLSm4; **E:** hLSm5; **F:** hLSm6; **G:** hLSm7; **H:** hLSm8. Arrowheads in **B** and **E** point out the faint cytoplasmic foci.

cytoplasmic foci. To demonstrate that these foci were identical to the ones that contain the endogenous hLSm1 and 4 proteins, we immunostained all transfected cells with hLSm1 and/or hLSm4 antibodies, and compared the localization by confocal microscopy. Figure 3 exemplarily shows that the YFP-hLSm6 foci (Fig. 3A) mostly overlap with those containing hLSm4 (Fig. 3B) and thus appear yellow in the overlay picture (Fig. 3C). Only a few minor foci contained more YFP-hLSm6 or endogenous hLSm4, thus appearing reddish or greenish.

The cytoplasmic foci contain hLSm heteromers

All Sm and LSm proteins investigated so far have been shown to function as heptamers (see Introduction). Therefore, we expected the cytoplasmic foci to contain hLSm heteromers. Because the Sm domain is both necessary and sufficient for the association of Sm/LSm proteins with one another, mutations in the Sm domain should prevent incorporation of the affected LSm protein into the foci. We chose hLSm4 to test this hypothesis, and introduced two point mutations ($G_{27}D$ and $L_{40}N$) in conserved residues of the Sm motif-I. The corresponding mutations have previously been shown to inhibit the interaction of yeast SmE with the SmF and SmG proteins (Camasses et al., 1998). The expression and integrity of the mutant proteins was verified by western blotting (data not shown). As shown in Figure 4, wild-type YFP-hLSm4 was incorporated into foci that overlapped with CFP-hLSm6 foci (Fig. 4A–C). In contrast, both YFP-hLSm4-$G_{27}D$ and YFP-hLSm4-$L_{40}N$ failed to accumulate in cytoplasmic foci; instead, they showed a homogeneous staining in the nucleus and the cytoplasm (Fig. 4D, G), as did the freely diffusible YFP molecule (data not shown). The localization of CFP-hLSm6 at the cytoplasmic foci, on the other hand, was not affected by expression of the mutant hLSm4 proteins (Fig. 4E, H). Thus, an intact Sm domain is needed for incorporation of hLSm4 into cytoplasmic foci. This finding suggests strongly that association of the LSm proteins is a necessary condition for the observed enrichment in these foci.

The idea that only hLSm protein complexes accumulate in the foci may also explain the fact that some of the tagged hLSm proteins accumulate only poorly (see above): Owing to their overexpression, they could simply lack binding partners. Therefore, we expressed every combination of YFP and CFP-tagged hLSm proteins pair-wise, and determined how the expression of one protein influenced the localization of the other. Because the foci become more readily visible after a longer time (30 h in Fig. 2), we expressed the pairs for a shorter time (12 h), in order to ensure more stringent conditions. The most striking effect was observed for the localization of YFP-hLSm2. Under the stringent conditions chosen, only very few of the transfected cells (4%) exhibited visible foci (Fig. 5A). However, upon coexpression of CFP-hLSm3 or CFP-hLSm6, a significant number of cells (37% and 83%, respectively) exhibited readily visible YFP-hLSm2 foci in the cytoplasm (Fig. 5B, C; note that only the YFP-hLSm2 fluorescence is shown). No other hLSm proteins showed this effect (exemplified by hLSm5; Fig. 5D). A similar, but less pronounced effect was observed with hLSm4, where coexpression of hLSm1 or hLSm4 increased the number of cells with YFP-foci from 29% to 53% and 83%, respectively, whereas coexpression of other hLSm proteins did not have any effect, and hLSm7 even reduced the number of foci (to 11%). The YFP-hLSm3 localization changes in a different way. This protein is incorporated into the foci even when expressed alone (Fig. 5E). Upon coexpression of CFP-hLSm2 and, above

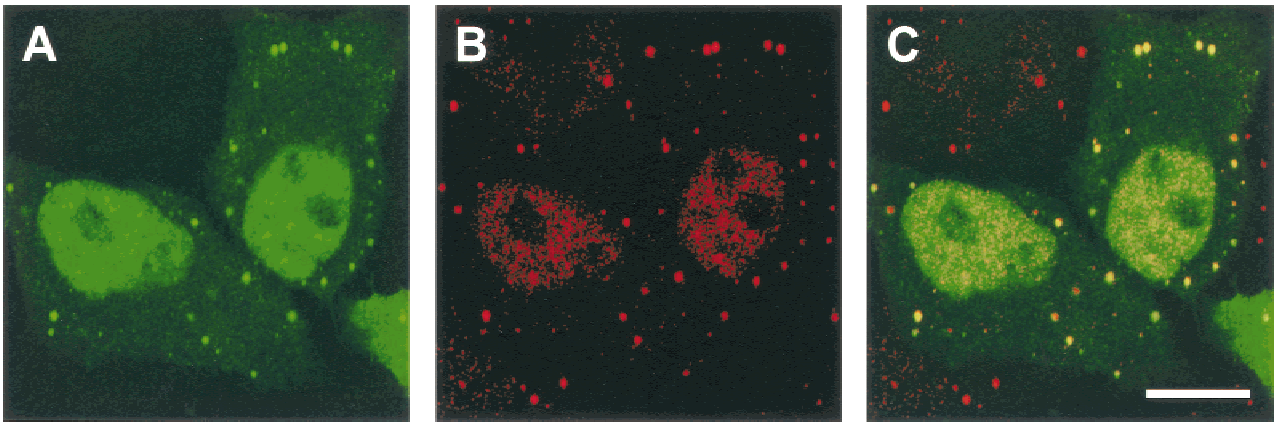

FIGURE 3. YFP-hLSm6 colocalizes with the endogenous hLSm proteins. HeLa cells expressing the YFP-LSm6 fusion protein were counterstained with anti-hLSm4 primary and Texas Red-conjugated secondary antibodies and visualized by confocal microscopy. Single sections of the YFP image (shown in green, left) and of the Texas-Red image (red, middle) are shown. In the overlay picture (right), overlap of the two signals appears yellow. Scale bar = 10 μm.

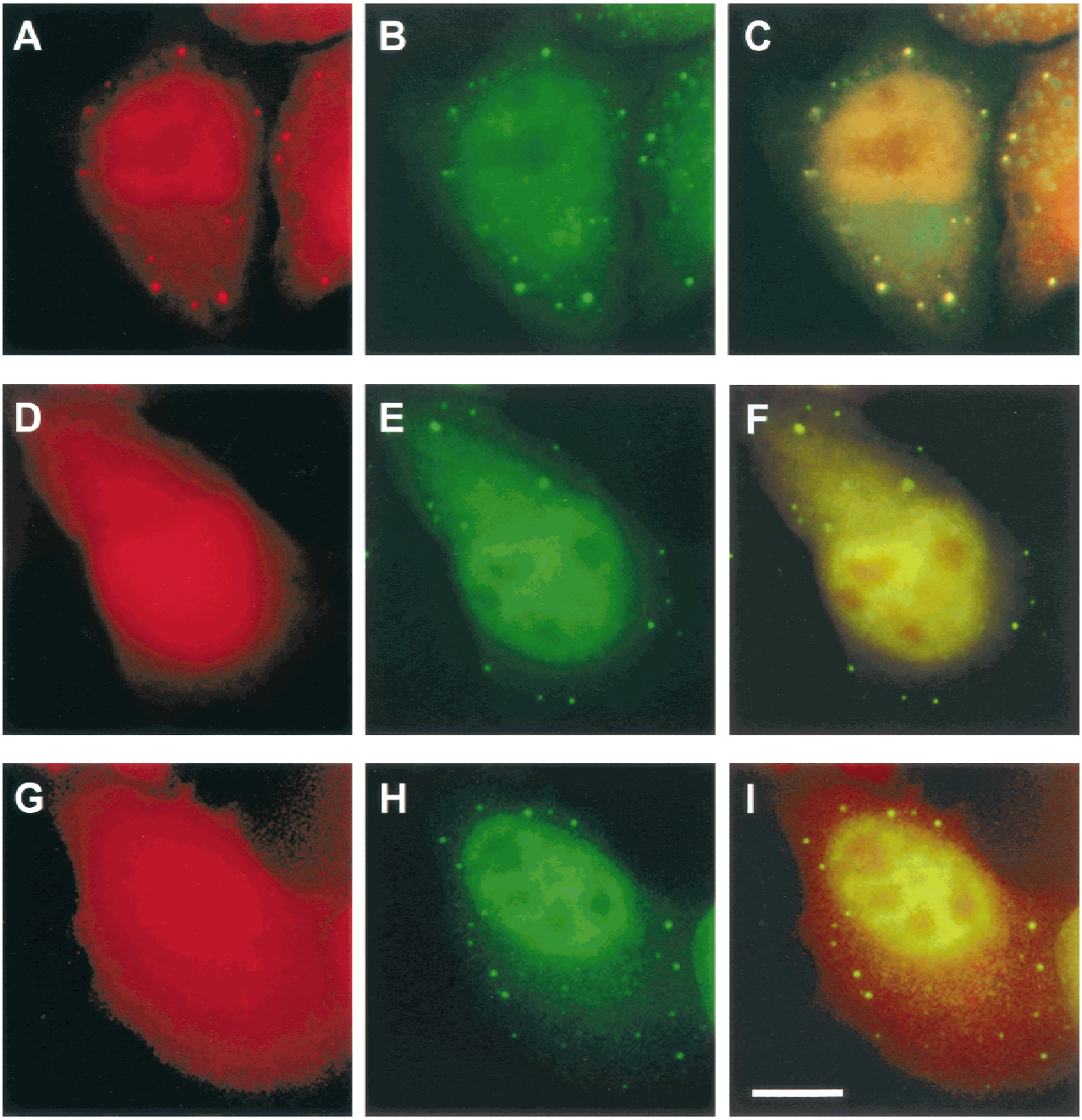

FIGURE 4. Mutations in the Sm domain abolish accumulation of YFP-hLSm4 in cytoplasmic foci. HeLa cells were transfected with CFP-hLSm6 plus the wild-type YFP-hLSm4 (**A**–**C**), the YFP-hLSm4 mutant $G_{27}D$ (**D**–**F**), or YFP-hLSm4 mutant $L_{40}N$ (**G**–**I**). The cells were fixed 12 h after transfection, and wide-field microscopic images were obtained. The YFP fluorescence is shown in red (**A**, **D**, **G**), and CFP in green (**B**, **E**, **H**). An overlay of both channels is shown in the right-hand column (**C**, **F**, **I**). Scale bar = 10 μm.

all, of CFP-hLSm6, the foci became significantly brighter (Fig. 5F, G) indicating that more YFP-hLSm3 protein was incorporated. Again, this effect appears to be specific, as no other hLSm protein changed the localization of YFP-hLSm3 (exemplified by CFP-hLSm4; Fig. 5H). Importantly, hLSm8 was never observed in cytoplasmic foci, neither when expressed alone (Fig. 2) nor in any combination with other hLSm proteins (data not shown).

In conclusion, we observe a general stimulation of hLSm protein incorporation when hLSm6 was coexpressed: only hLSm8 was not influenced. In addition, there was a specific enhancement of the hLSm2/3 (Fig. 5B, F), and the hLSm1/4 pairs (data not shown). Furthermore, hLSm6 appeared to have a stronger effect on hLSm3 than on any other hLSm protein, as gauged by the amount of protein incorporated into the foci (Fig. 5G).

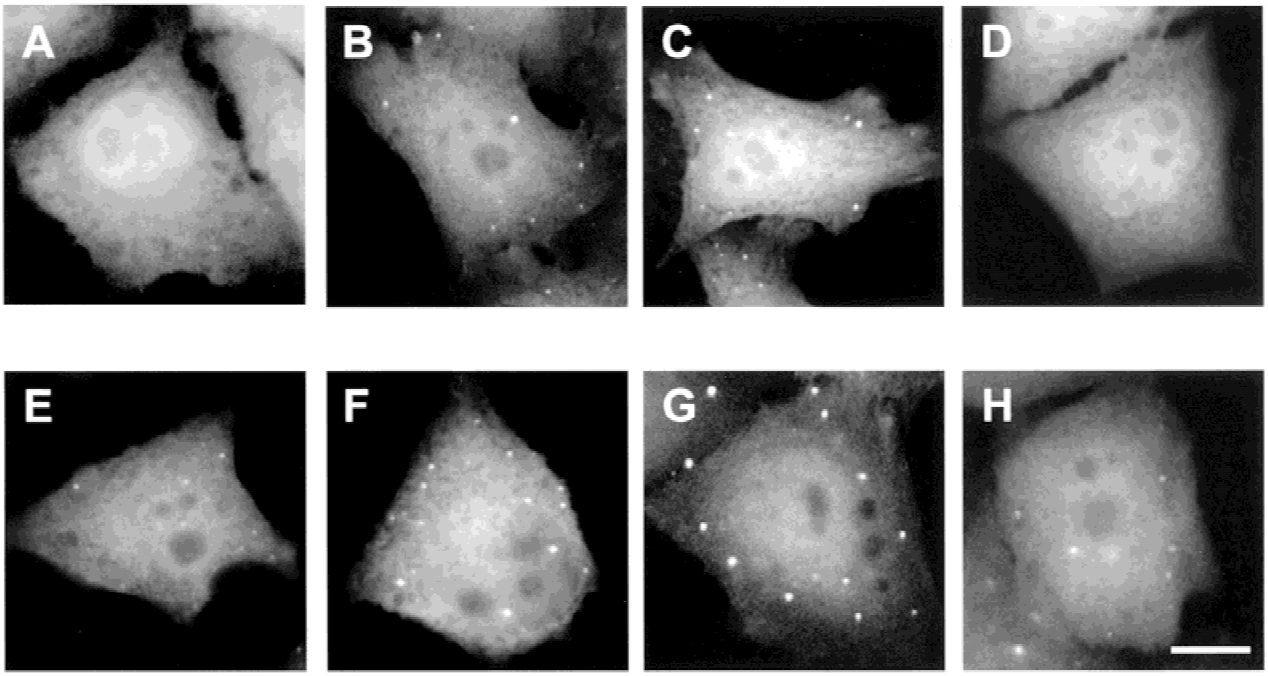

FIGURE 5. Coexpression of certain hLSm pairs enhances their incorporation into cytoplasmic foci. HeLa cells were fixed 12 h after expression of YFP-hLSm2 alone (**A**) or YFP-LSm2 coexpressed with CFP-hLSm3 (**B**), CFP-hLSm6 (**C**), and CFP-hLSm5 (**D**). The lower row shows expression of YFP-hLSm3 alone (**E**), or YFP-hLSm3 coexpressed with CFP-hLSm2 (**F**), CFP-hLSm6 (**G**), and CFP-hLSm4 (**H**). In all panels, only the YFP fluorescence is shown. Scale bar = 10 μm.

To determine whether the presumed protein pairs hLSm1/4, hLSm2/3, and hLSm3/6 indeed formed molecular complexes in vivo, we performed fluorescence resonance energy transfer (FRET) measurements. The fluorescent protein pairs of CFP and YFP can serve as donor and acceptor, respectively, with a calculated Förster distance, R_0, of 4.9 nm for unoriented molecules (Patterson et al., 2000). Owing to the presence of endogenous hLSm proteins in the cells and the variable expression of the FP-hLSm constructs, it is not possible to demonstrate FRET unambiguously by using sensitized acceptor emission alone. However, the FRET efficiency can be measured by acceptor photobleaching. This method makes use of the fact that FRET quenches the donor fluorescence as the excitation energy is transferred to the acceptor. After photobleaching of the acceptor, this quenching no longer occurs, and the donor fluorescence increases. Quantification of the increase is a reliable and robust measure of FRET (Bastiaens & Jovin, 1997; Miyawaki & Tsien, 2000).

In all cells expressing FP-tagged hLSm6 and hLSm3, we measured a positive FRET efficiency of 20–33% in both the cytoplasm and the foci, as shown in Figure 6A. Similar values were observed in cells expressing both FP-tagged hLSm2 and hLSm3 (Fig. 6B). It should be noted, however, that in this case only 50% of the transfected cells showed FRET; the others showed no effect. This may possibly reflect various levels of endogenous hLSm protein expression (see Discussion). Moreover, FRET was absent with the pair hLSm4 and hLSm1, even when hLSm6 was coexpressed to induce the formation of strong cytoplasmic foci (Fig. 6C). Similarly, we saw no energy transfer between the FP-tagged hLSm6 and hLSm4 (Fig. 6D). In the cases of the hLSm2/3 pair and the hLSm1/4 pair, we exchanged the donor and acceptor fluorescent fusion moieties, with the same results.

Finally, we confirmed the FRET data by using an entirely different method, that of fluorescence lifetime imaging (Clegg et al., 1994; Bastiaens & Squire, 1999; Miyawaki & Tsien, 2000; Hanley et al., 2001). FRET is accompanied by a decreased lifetime of the donor, reflecting its quenching. Because of the large variation in expression levels of the tagged pairs, the FLIM measurements do not yield a single average lifetime for the donor in the different cells. However, the lifetimes in photobleached areas were distinctly longer than before the bleaching, and were similar to those obtained in cells expressing only the CFP-LSm fusion proteins. These results confirmed the existence of FRET in the hLSm2/3 and hLSm3/6 expression pairs. There was no change in the donor lifetime upon bleaching cells expressing the hLSm1/4 pair, confirming the absence of FRET that we had observed by the acceptor-photobleaching technique. We conclude that certain pairs of hLSm proteins are in molecular contact with each other, and that coexpression of these pairs en-

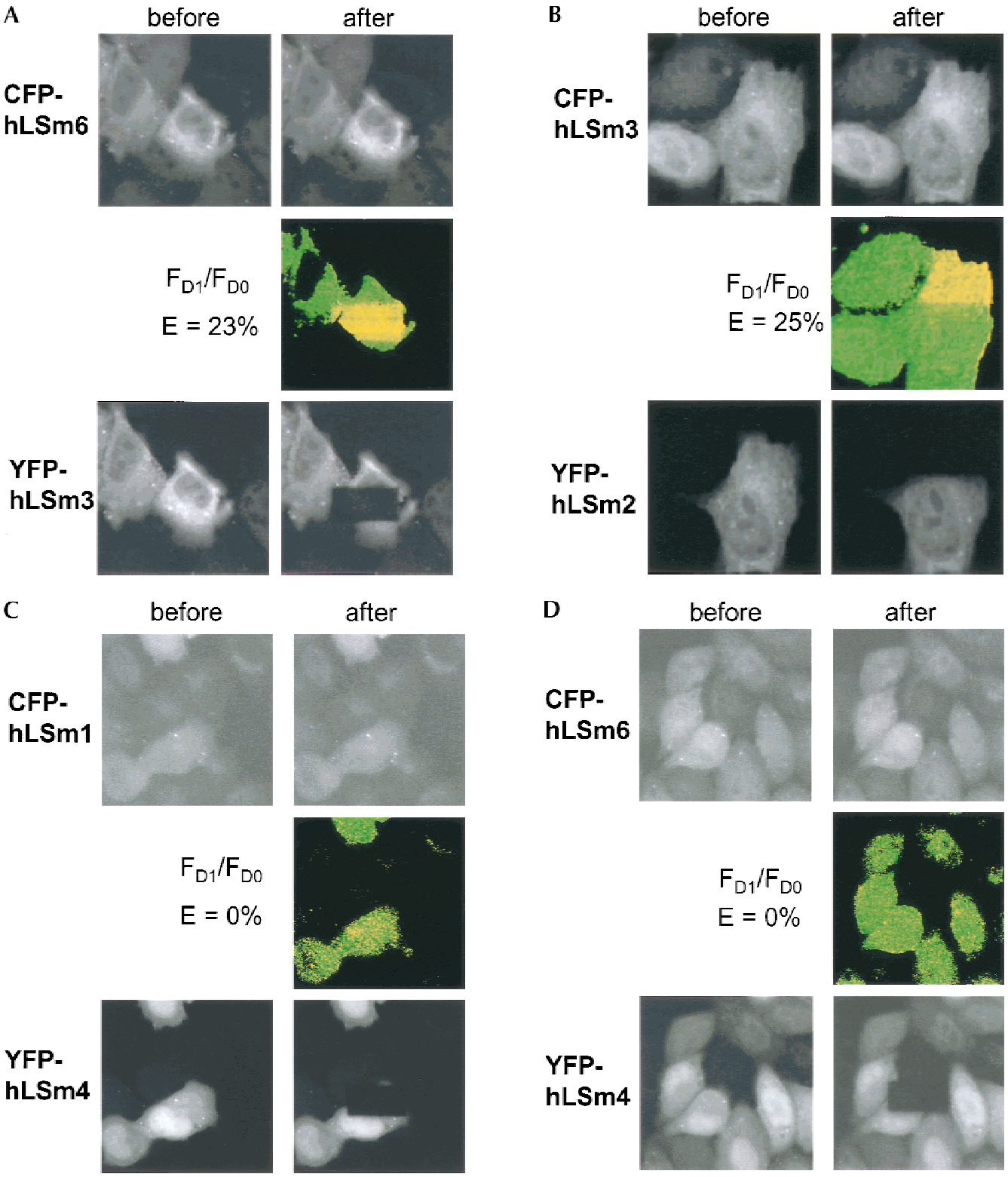

FIGURE 6. hLSm proteins interact directly in vivo as demonstrated by FRET. The following hLSm pairs were coexpressed: CFP-hLSm6/YFP-hLSm3 (**A**), CFP-hLSm3/YFP-hLSm2 (**B**), CFP-hLSm1/YFP-hLSm4 (**C**), and CFP-hLSm6/YFP-hLSm4 (**D**). The cells were fixed 15 h after transfection, mounted, and confocal images of both CFP and YFP channels were taken before and after photobleaching. The intensity of the CFP-fluorescence after photobleaching (F_{D1}) was divided by the CFP-fluorescence before photobleaching (F_{D0}). The ratio was calculated pixel by pixel, and the result is shown color coded. Green indicates a ratio of 1 (no increase), yellow a ratio greater than 1 (positive increase). *E* is the mean value for the calculated energy transfer efficiency.

hances their incorporation into the cytoplasmic foci. It is important to note, however, that the FRET efficiency, and hence the ratio of heteromers over monomers, seems to be the same in the foci and in other parts of the cytoplasm (see Discussion).

The cytoplasmic foci also contain high concentrations of key mRNA-degrading factors

The data presented above imply that the proteins hLSm1–7 form a complex with a cytoplasmic function. The yeast homologs of these proteins have been shown to form a complex that participates in mRNA degradation and associates with the decapping enzyme Dcp1p and with the exonuclease Xrn1p (see Introduction). To see whether this function is conserved between species, we investigated whether other factors of the mRNA degradation pathway are also present in the hLSm foci. The mammalian homolog of the endonuclease Xrn1 has been found in the cytoplasm, where it becomes localized in a diffuse pattern and is, interestingly, also enriched in a few cytoplasmic foci (Bashkirov et al., 1997). To elucidate whether the foci of hXrn1 and hLSm enrichment are indeed the same, we used the monoclonal anti-mXrn1 antibody (Bashkirov et al., 1997). On western blots of HeLa cell extracts, this antibody recognized a single protein of the appropriate size, indicating that the Xrn1 protein, and especially the epitope of the antibody, is conserved between mouse and man (H. Brahms & R. Lührmann, pers. comm.). Immunostaining with hLSm antibodies showed that hLSm4 cytoplasmic foci (Fig. 7A) coincide with the foci of hXrn1 enrichment (Fig. 7B). In contrast, the hLSm protein staining pattern does not overlap with Xrn1 in the diffuse pattern outside of the foci.

The human homologs of the yeast decapping enzymes Dcp1p and Dcp2p have been characterized only recently (J. Lykke-Anderson, 2002). To elucidate whether the two proteins are also enriched in the cytoplasmic foci, we transiently expressed FLAG-tagged versions of the proteins (J. Lykke-Anderson, 2002) in HeLa cells. The cells were stained with anti-FLAG and anti-hLSm1 antibodies. The result is shown in Figure 8: Both proteins are distributed throughout the cytoplasm. In addition, many transfected cells show a clear enrichment of hDcp1 and hDcp2 in several cytoplasmic foci (Fig. 8A, D). Importantly, the hDcp1 and hDcp2 foci nicely coincide with the foci stained by hLSm1 antibodies (Fig. 8B–C, E–F), indicating that they are again identical. Thus, the hDcp staining pattern closely resembles the pattern obtained by anti-Xrn1 staining. The fact that not all transfected cells exhibit hDcp foci may indicate that the level of overexpression affects the incorporation of the hDcp proteins into native complexes as observed for the hLSm proteins (see above). We conclude that the foci contain, in addition to the hLSm proteins, the exonuclease hXrn1 and both subunits of the decapping enzyme hDcp; the foci are therefore linked to mRNA degradation (see Discussion).

DISCUSSION

The hLSm proteins 1–7 colocalize with key mRNA-degrading enzymes in cytoplasmic foci

Whereas the Sm-like proteins LSm2 to 8 form a nuclear complex that takes part in the pre-mRNA splicing, the LSm1 to 7 proteins form, at least in yeast, a largely overlapping complex that migrates to the cytoplasm, where it has a function in mRNA degradation (see In-

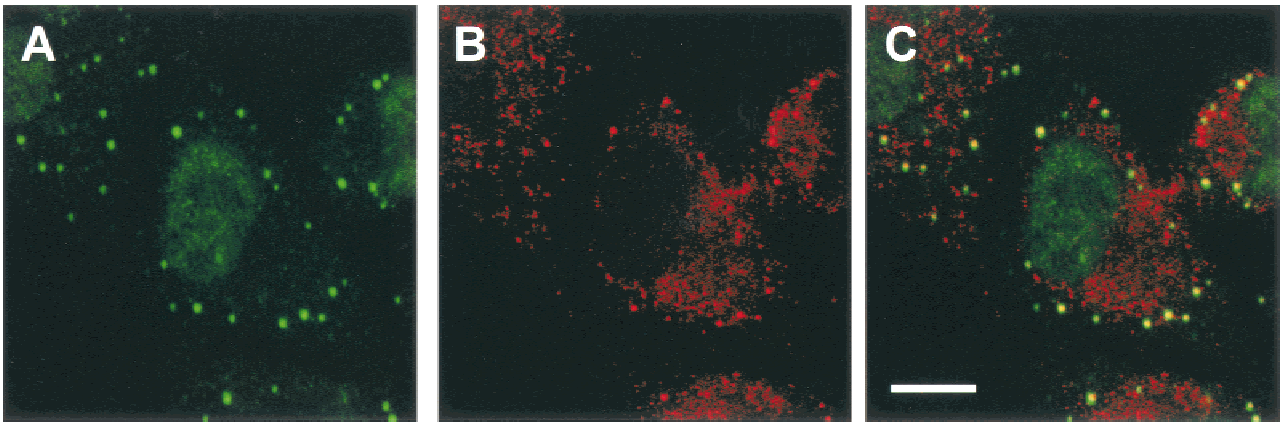

FIGURE 7. hLSm4 is colocalized with hXrn1 in cytoplasmic foci. HeLa cells were grown on cover slips, fixed, and double labeled by indirect immunofluorescence with affinity-purified rabbit anti-hLSm4 and monoclonal mouse anti-mXrn1 antibodies. The confocal sections of hLSm4 (**A**) are shown in green (Alexa488-conjugated secondary antibody), and hXrn1 (**B**) in red (Texas-Red-conjugated secondary antibody). In the overlay picture (**C**), overlap of the colors appears yellow. Scale bar = 10 μm.

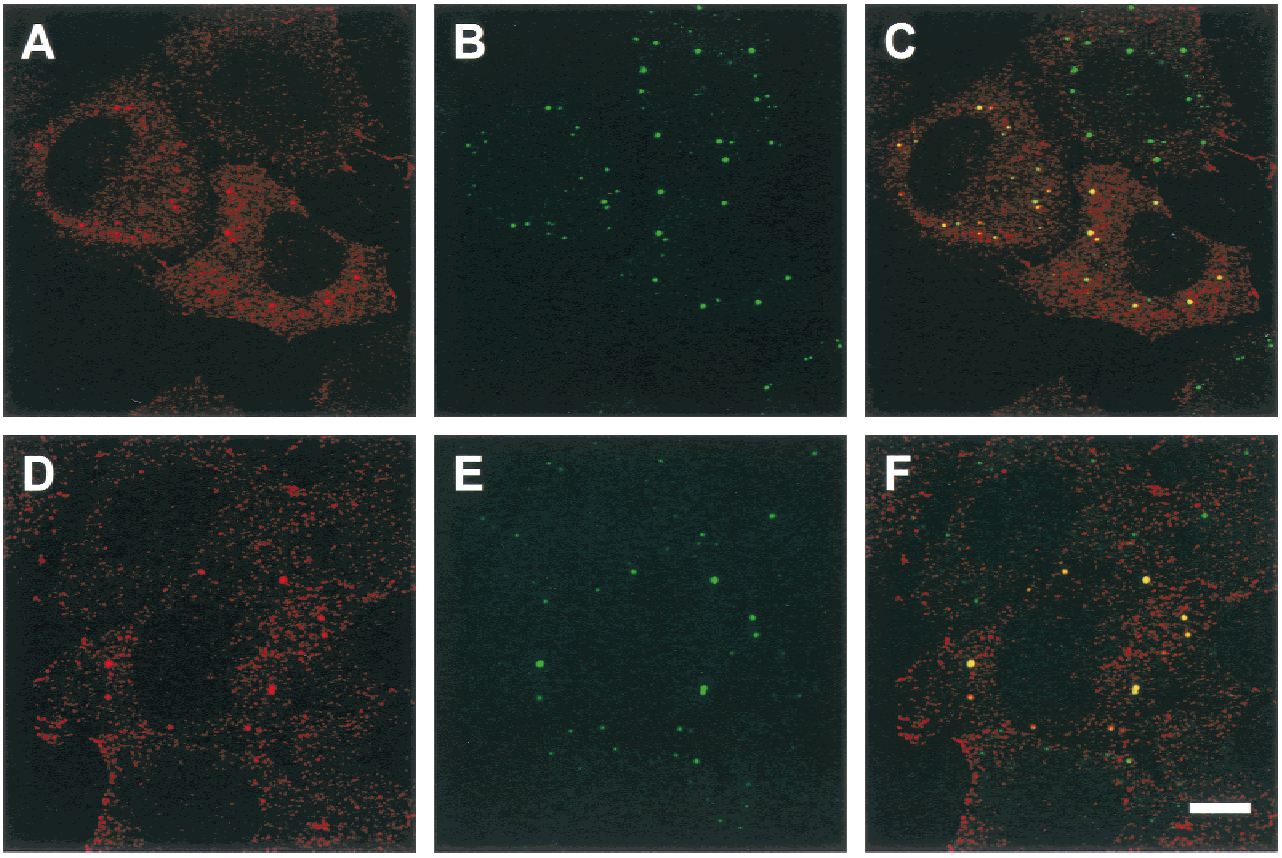

FIGURE 8. hLSm1 is colocalized in cytoplasmic foci with the two subunits of the decapping enzyme. HeLa cells were grown on cover slips and transfected with plasmids encoding FLAG-tagged versions of the proteins hDcp1 (**A**–**C**) and hDcp2 (**D**–**F**). The cells were then fixed and double labeled by indirect immunofluorescence with affinity-purified rabbit anti-hLSm1 and monoclonal mouse anti-FLAG antibodies. The confocal sections of hLSm1 (**B**, **E**) are shown in green (Alexa488-conjugated secondary antibody), and the FLAG-tag (**A**, **D**) in red (Texas-Red-conjugated secondary antibody). In the overlay picture (**C**, **F**), overlap of the colors appears yellow. Scale bar = 10 μm.

troduction). Here, we characterize the apparent human homolog of LSm1 and show that all proteins hLSm1–7 are highly enriched in multiple foci distributed throughout the cytoplasm (Figs. 1, 2, and 3). hLSm8, in contrast, is not found in these foci (Fig. 2). A little caveat remains, as hLSm8 was overexpressed as an FP-tagged version, and the tag may have interfered with the function and/or localization of the protein. Antibodies raised against the hLSm8 protein exhibited, unfortunately, strong cytoplasmic cross-reactions. Still, they did not reveal enrichment of the hLSm8 protein in cytoplasmic foci, whereas the similarly cross-reacting hLSm7 antibodies did (data not shown). Therefore, we conclude that the proteins LSm1–7, but not LSm8, accumulate specifically in the cytoplasmic foci. The human LSm1 protein, like its yeast counterpart, is thus linked to LSm2–7. Furthermore, several lines of evidence indicate that proteins hLSm1 to 7 indeed form a protein complex (see below).

In addition to the hLSm proteins, the cytoplasmic foci contain high concentrations of two key factors required for the 5′-to-3′ mRNA decay, namely the two subunits of the decapping enzyme hDcp (Fig. 8) and the exonuclease hXrn1 (Fig. 7). This strongly links the cytoplasmic foci—and hence the human proteins LSm1–7—to mRNA degradation. Thus, these results show that the involvement of the LSm proteins in mRNA degradation is conserved throughout the eukaryotic kingdoms. However, the striking enrichment of the factors in cytoplasmic foci is not observed in yeast (Tharun et al., 2000). The function of the foci remains to be elucidated. Whatever the function of the cytoplasmic foci, it is important to note that they are not restricted to human HeLa cells: We have observed similar hLSm1 foci in monkey kidney (COS-7) and mouse fibroblast (3T3) cells (data not shown). Therefore, appearance of the LSm1 foci is not a unique feature of the HeLa cells; it remains to be seen, however, whether cells that are not immortalized also exhibit the LSm foci.

It can be imagined that the foci function as assembly centers, storage sites, and/or places where mRNA degradation actually takes place. We see preliminary hints for a function as assembly/storage sites, but it is also possible that mRNA is degraded in the foci. Thus, the

Xrn1 nuclease is found not only in the LSm foci, but also in a more diffuse cytoplasmic pattern (Bashkirov et al., 1997). Likewise, both subunits of the decapping enzyme hDcp are distributed all over the cytoplasm. The fact that hLSm1 is found predominantly, if not exclusively, in the foci (Figs. 1 and 2) could indicate that the degradation machinery is assembled and/or stored in the foci, whereas the degradation takes place in the cytoplasm. Alternatively, there could be two pathways for the 5′-to-3′ mRNA decay, of which only one requires the hLSm proteins.

The results from overexpression of pairs of LSm proteins seem to suggest that subcomplexes of the heptamer can enter the foci (see below), which in turn would support the idea that the LSm heptamers are assembled there. In vitro, hLSm4 interacts through its RG-rich C terminus with the Sm assembly factor SMN (Brahms et al., 2001; Friesen et al., 2001). Because SMN is not enriched in cytoplasmic foci (Liu et al., 1997), this would argue against hLSm assembly in the foci. However, it is important to note that deletion of the RG-rich C-terminus—the SMN interaction domain—does not prevent hLSm4 from appearing in the cytoplasmic foci (data not shown). Thus it remains to be seen, in future studies, whether SMN participates in the assembly of hLSm1–7 complexes, and where this process takes place.

The cytoplasmic foci contain assembled complexes

Several lines of evidence indicate that the cytoplasmic foci contain assembled complexes rather than just high concentrations of the monomeric proteins. First of all, the folding of the Sm domain, rather than the presence of isolated signal peptides is essential for accumulation of the hLSm proteins in the cytoplasmic foci. Thus, point mutations of highly conserved amino acids in the Sm domain of hLSm4 abolished the localization of this protein in cytoplasmic foci (Fig. 4). The mutated residues make a crucial contribution to the folding of the Sm domain (Kambach et al., 1999; Collins et al., 2001; Mura et al., 2001; Törö et al., 2001), and it is therefore likely that the mutated Sm domains no longer fold correctly. Because the Sm domain is necessary for complex formation among members of the Sm protein family, the mutant proteins presumably fail to interact with other Sm/LSm proteins, as demonstrated for the corresponding mutants of the yeast SmE protein (Camasses et al., 1998). This also agrees with the fact that the expression of mutant hLSm4 proteins does not have a dominant negative effect on the accumulation of hLSm6 in the foci. Thus, these mutations suggest that the interaction of hLSm4 with other hLSm proteins is necessary for the enrichment of this protein in the cytoplasmic foci.

Next, overexpression of the hLSm6 protein led to a very efficient incorporation into the cytoplasmic foci, whereas other hLSm proteins were incorporated more slowly and/or to a lesser extent. Coexpression of hLSm6, however, increased the appearance of all other hLSm proteins—except hLSm8—in the foci. This result can best be explained by assuming that the foci contain functional, heptameric hLSm1–7 complexes and that hLSm6 is the limiting factor for hLSm complex formation in HeLa cells. Interestingly, certain other combinations of hLSm proteins also stimulated their appearance in cytoplasmic foci (Fig. 5). This was most evident for the hLSm2 protein which, when expressed alone, hardly appeared in the foci. In this case, coexpression not only of hLSm6, but also of hLSm3 strongly increased the accumulation of hLSm2 in the foci. In addition, the hLSm3/hLSm6 pair showed a very strong accumulation in the foci, and the proteins hLSm1 and hLSm4 showed some mutual stimulation of their incorporation in the foci. Because the proteins are expressed in excess over the endogenous proteins (estimated for hLSm1 and 4 by western blotting; data not shown), this may signify that hLSm dimers form, and that these can enter the foci. Subcomplexes of two or three Sm proteins have been observed (Raker et al., 1996), but such complexes have not yet been described for the LSm proteins. In fact, the arrangement of the LSm proteins in the heptameric complex has not yet been elucidated.

Finally, proof that the hLSm2/3 and hLSm3/6 pairs are indeed very closely associated in vivo comes from FRET imaging (Fig. 6). The distance at which the cyan and yellow fluorescent proteins should elicit 50% energy transfer (R_0) is 4.9 nm, and this function varies with the inverse sixth power of the distance (Förster, 1951). Thus, because the FP-fusion LSm proteins are expected to form a ring structure of approximately 8 nm diameter with the FP moieties at the periphery (Kambach et al., 1999), we should be able to observe transfer from nearest-neighbor pairs, but not from pairs that span the ring (note that the size of the FP moieties prevents the two chromophores from approaching one another to a distance of less than 2 nm). The stringent distance requirements allow us to probe neighbor pairs in the complex. The consistent energy transfer efficiency of 23–33% observed for the CFP-LSm6 and YFP-LSm3 pair indicates a close association between the labeled proteins. Also, the fact that all cells expressing both proteins that were measured showed a positive energy transfer efficiency suggests that the complex was not significantly diluted with unlabeled endogenous hLSm proteins, which would have reduced the efficiency of the FRET. The data thus support the hypothesis that hLSm6 may be limiting for ring formation, so that other exogenously expressed hLSm proteins are incorporated into complexes containing predominantly labeled hLSm6. The CFP-hLSm3 and YFP-hLSm2 pair gave an energy transfer efficiency of 15–

30% in some cells, clearly indicating complex formation, whereas in others it showed no transfer. We believe that these results may be explained by less efficient expression of the proteins in some cells compared to the level of the endogenous proteins, and/or the wide variety of expression levels in the transiently transfected cells. This could also explain that, in the same preparation, some cells exhibit foci containing FP-LSm while other cells with similar expression levels do not.

Although the arrangement of the LSm proteins in the ring is not yet known, it is interesting to note that, among the Sm proteins, the closest homologs of the LSm proteins 2, 3, and 6 are the Sm proteins D1, D2, and F (Achsel et al., 1999; Salgado-Garrido et al., 1999). These three proteins happen to be neighbors in the Sm ring (Kambach et al., 1999, and references therein), suggesting that the LSm proteins are arranged in the LSm ring in the same order as their closest homologs are in the Sm ring. This idea is also supported by yeast data showing that the yLsm proteins 4-8-2 interact genetically (Pannone et al., 2001). Furthermore, yeast two-hybrid analysis showed strong, reciprocal interactions between the yLsm2 and 8 (Mayes et al., 1999; Fromont-Racine et al., 2000) and the yLsm5–7 and 6–7 pairs (Fromont-Racine et al., 2000). In each case, the homologous Sm proteins are neighbors on the Sm ring. According to this model, LSm1 and 4 should also be neighbors and interact with each other, and indeed we observed a weak stimulation of hLSm4 incorporation into the cytoplasmic foci when hLSm1 is coexpressed; however, FRET was not observed. Because hLSm6 promotes incorporation of other hLSm proteins into the foci, we reasoned that triple expression of hLSm1/4 plus hLSm6 might yield a stronger incorporation and hence association of the hLSm1/4 pair. Because acceptor photobleaching is not sensitive to an excess of free acceptor, we chose YFP-hLSm6 when the YFP-hLSm4/CFP-hLSm1 interaction was measured. No FRET was observed, suggesting that hLSm1 is not in the close vicinity of hLSm4 nor hLSm6. It should be noted, however, that FRET interactions even of close neighbors may be undetectable for several reasons, for example, when the dipole moments of the chromophores are perpendicular, or when the ratio of endogenous to exogenous protein is too large to permit efficient FP pair formation.

We conclude that the cytoplasmic foci contain assembled, functional LSm complexes. Moreover, FRET imaging demonstrates that the complexes are not confined to the foci. In fact, there is no difference in FRET efficiency between the foci and the surrounding cytoplasm (Fig. 6) indicating that the ratio between complexed and free LSm proteins is the same in both compartments. The results are compatible with complex assembly immediately after translation and subsequent migration to the foci; however, alternatively, the assembled complexes may shuttle between the foci and the cytoplasm.

Subcellular targeting of the LSm proteins

The presence of human LSm proteins in both the cytoplasmic and nuclear compartments raises the interesting question of how the cell specifically targets overlapping sets of LSm proteins to various locations. The hLSm1–7 complex is targeted with high efficiency to the cytoplasmic foci, whereas the hLSm2–8 complex migrates, as part of the splicing machinery, to the nucleus (Fig. 1) and there to the respective nuclear bodies. Thus, the replacement of hLSm1 by hLSm8 not only redirects the complex to the nucleus, it also leads to its accumulation in entirely different subcellular structures. This is remarkable, because hLSm1 and hLSm8 are highly homologous to each other. In fact, they are more closely related to each other than to any other Sm or LSm protein (Achsel et al., 1999). The only striking difference between the two proteins is a C-terminal extension of 33 amino acids that is found only in hLSm1. Preliminary experiments indicate that this peptide is necessary, but not sufficient, for the proper localization of hLSm1. Furthermore, it is not even known whether the individual proteins or the assembled hLSm complexes are targeted to the nucleus and the cytoplasmic foci, respectively. It will therefore be interesting to elucidate, in future experiments, which features in the LSm1 and 8 proteins are responsible for the highly specific targeting, and which factor(s) recognize these features.

MATERIALS AND METHODS

Plasmid constructs

The vectors pECFP-C1 and pEYFP-C1 (Clontech) encoding an enhanced cyan fluorescent (CFP) and an enhanced yellow fluorescent (YFP) variant of the *Aequorea victoria* green fluorescent protein (GFP) gene, respectively, were modified to contain in-frame *Hin*dIII and *Eco*RI cloning sites. The human LSm1–8 ORFs were amplified by PCR from their ESTs (Achsel et al., 1999) and the resulting PCR fragments were subcloned into the *Hin*dIII/*Eco*RI restriction sites of the vectors. Integrity of the inserts was verified by dideoxy sequencing.

Cell culture, transient transfection, and fluorescence microscopy

HeLa SS6 cells were grown on glass cover slips (Fisher Scientific) in Dulbecco's modified Eagle's medium (GibcoBRL) supplemented with 10% foetal calf serum (GibcoBRL) and 100 U/mL penicillin/streptomycin (Biochrom KG) at 37 °C, 5% CO_2. Transfections were performed after cells had reached ~80% confluence by using LipofectAMIN^{TM} 2000 (GibcoBRL) under conditions recommended by the manufacturers. After incubation, the cells were washed in PBS, fixed for 20 min with 4% (w/v) paraformaldehyde/1× PBS, pH 7.4, and mounted in antifade (Mowiol, Calbiochem). Samples were visualized using a 63×/1.4 N.A. objective of a Leica DM/IRB inverted wide-field fluorescence microscope and digitized images were taken with a cooled charge-coupled device cam-

era (Visitron Systems). To exclude bleed-through in double-labeling experiments, filter sets (Chroma Technology) optimized for YFP and CFP excitation/emission spectra were used. Confocal images were obtained on a Leica TCS SP2 or Zeiss LSM 410 inverted confocal laser scanning microscope. To avoid bleed-through, the fluorophores were excited separately using standard laser lines. Fluorescence signals were acquired in 0.5-μm optical sections.

Immunofluorescence

In this study, polyclonal rabbit antibodies were used against hLSm1 (see below) and hLSm4 (Achsel et al., 1999), and mouse monoclonal antibodies against mXrn1 (Bashkirov et al., 1997), and the FLAG tag (M2, Sigma). Anti-LSm1 antibodies were raised by immunizing rabbits with the last 20 amino acids of hLSm1 coupled to BSA. Both the anti-hLSm1 and anti-hLSm4 antibodies were purified by binding to their epitope peptide immobilized on a Sulfolink gel (Pierce) and eluting at pH 2.7. In Figure 1, the purified antibodies were coupled to the fluorescent dyes using the AlexaFluor488 (Molecular Probes) and FluoroLink™ Cy3 labeling kits (Amersham), respectively, as recommended by the manufacturers. The following secondary antibodies were used: Texas Red goat anti-mouse and goat Alexa 488 anti-rabbit IgG (H+L) conjugates from Molecular Probes (1:500 dilution).

Cells were grown and fixed with PFA as described above, washed with PBS, and permeabilized in 0.2% Triton X-100 (Sigma) for 20 min. Cells were then rinsed with PBS, blocked in PBS/10% FCS for 30 min and incubated with the primary antibody diluted in PBS/10% FCS for 60 min. Subsequently, cells were washed with PBS (4 $\times$ 15 min) and incubated with the secondary antibody diluted in PBS/10% FCS for 45 min. The cells were washed again with PBS (4 $\times$ 15 min) and mounted in antifade (Mowiol, Hoechst). All steps were performed at room temperature.

Acceptor photobleaching FRET

All data were obtained on a LSM 310 (Zeiss, Jena) modified with an external argon-ion 5-W laser (Spectra Physics, Palo Alto, CA) tuned to 457.8 nm and coupled by a monomode optical fiber. Samples were mounted in Mowiol and images acquired with a 63$\times$ 1.4 N.A. oil-immersion Apo-chromat lens. Specific excitation and emission of the LSm proteins fused to CFP was effected by excitation at 457.8 nm and collection of emitted light with a 495-nm HW 20-nm bandpass filter (Omega Brattleboro, VT). No emission from YFP fusion proteins was detected in this channel. CFP images were taken before and after photobleaching of the YFP signal by using exactly the same sensitivity settings. YFP signals were photobleached by full power excitation at 514 using an 8-mW argon-ion laser. Images of the LSm-YFP expressing cells were obtained before and after photobleaching by excitation with 100-fold attenuated 514-nm excitation and emission collected from 530 to 585 nm (Delta Light and Optics, Denmark). No photobleaching of the CFP signal was observed under conditions of $>$90% photodestruction of the YFP signal. FRET efficiencies were calculated by using algorithms as described (Bastiaens & Jovin, 1997) using the computer software Scilimage (Delft, Netherlands).

Fluorescence lifetime imaging

The homodyne fluorescence lifetime imaging microscope has been described elsewhere (Clegg et al., 1994; Hanley et al., 2001). The excitation light and the intensifier gain were modulated at 59 MHz. Excitation was effected by a 5-W argon-ion laser (Coherent, Palo Alto, CA) tuned to 457.8 nm, and emission was collected by using a notch filter (Kaiser Optical Systems, Ann Arbor, MI) to eliminate excitation light and a bandpass filter at 470 nm HW 30 (Omega). Eight phases were collected bidirectionally, and lifetimes were calculated from both phase and modulation data by Fourier transform algorithms using a rhodamine 6G solution as a standard (Hanley et al., 2001).

ACKNOWLEDGMENTS

We thank V. Bashkirov for anti-Xrn1 antibodies, J. Lykke-Andersen for plasmids encoding the tagged hDcp1 and hDcp2 proteins, and J. Lykke-Andersen and H. Brahms for sharing data prior to publication. This work was supported by a grant of the Deutsche Forschungsgemeinschaft (SFB523/A8) to R.L.

Received August 12, 2002; returned for revision September 5, 2002; revised manuscript received September 16, 2002

REFERENCES

Achsel T, Brahms H, Kastner B, Bachi A, Wilm M, Lührmann R. 1999. A doughnut-shaped heteromer of human Sm-like proteins binds to the 3′-end of U6 snRNA, thereby facilitating U4/U6 duplex formation in vitro. *EMBO J 18*:5789–5802.

Achsel T, Stark H, Lührmann R. 2001. The Sm domain is an ancient RNA-binding motif with oligo(U) specificity. *Proc Natl Acad Sci USA 98*:3685–3689.

Bashkirov VI, Scherthan H, Solinger JA, Buerstedde JM, Heyer WD. 1997. A mouse cytoplasmic exoribonuclease (mXRN1p) with preference for G4 tetraplex substrates. *J Cell Biol 136*:761–773.

Bastiaens PI, Jovin TM. 1997. Fluorescence resonance energy transfer (FRET) microscopy. In: Elis JE, ed. *Cell biology: A laboratory handbook*. New York: Academic Press.

Bastiaens PI, Squire A. 1999. Fluorescence lifetime imaging microscopy: Spatial resolution of biochemical processes in the cell. *Trends Cell Biol 9*:48–52.

Boeck R, Lapeyre B, Brown CE, Sachs AB. 1998. Capped mRNA degradation intermediates accumulate in the yeast spb8-2 mutant. *Mol Cell Biol 18*:5062–5072.

Bouveret E, Rigaut G, Shevchenko A, Wilm M, Séraphin B. 2000. A Sm-like protein complex that participates in mRNA degradation. *EMBO J 19*:1661–1671.

Brahms H, Meheus L, de Brabandere V, Fischer U, Lührmann R. 2001. Symmetrical dimethylation of arginine residues in spliceosomal Sm protein B/B′ and the Sm-like protein LSm4, and their interaction with the SMN protein. *RNA 7*:1531–1542.

Brahms H, Raymackers J, Union A, de Keyser F, Meheus L, Lührmann R. 2000. The C-terminal RG dipeptide repeats of the spliceosomal Sm proteins D1 and D3 contain symmetrical dimethylarginines, which form a major B-cell epitope for anti-Sm autoantibodies. *J Biol Chem 275*:17122–17129.

Brewer G. 1998. Characterization of c-myc 3′ to 5′ mRNA decay activities in an in vitro system. *J Biol Chem 273*:34770–34774.

Camasses A, Bragado-Nilsson E, Martin R, Séraphin B, Bordonné R. 1998. Interactions within the yeast Sm core complex: From proteins to amino acids. *Mol Cell Biol 18*:1956–1966.

Chen CY, Gherzi R, Ong SE, Chan EL, Raijmakers R, Pruijn GJ, Stoecklin G, Moroni C, Mann M, Karin M. 2001. AU binding pro-

teins recruit the exosome to degrade ARE-containing mRNAs. *Cell 107*:451–464.
Clegg RM, Gadella TWJ Jr, Jovin TM. 1994. Lifetime-resolved fluorescence imaging. *Proc SPIE*, 105–118.
Collins BM, Harrop SJ, Kornfeld GD, Dawes IW, Curmi PM, Mabbutt BC. 2001. Crystal structure of a heptameric Sm-like protein complex from archaea: Implications for the structure and evolution of snRNPs. *J Mol Biol 309*:915–923.
Fischer U, Liu Q, Dreyfuss G. 1997. The SMN-SIP1 complex has an essential role in spliceosomal snRNP biogenesis. *Cell 90*:1023–1029.
Förster T. 1951. *Fluoreszenz organischer Verbindungen*. Göttingen: Vandenhoeck.
Friesen WJ, Massenet S, Paushkin S, Wyce A, Dreyfuss G. 2001. SMN, the product of the spinal muscular atrophy gene, binds preferentially to dimethylarginine-containing protein targets. *Mol Cell 7*:1111–1117.
Fromont-Racine M, Mayes AE, Brunet-Simon A, Rain JC, Colley A, Dix I, Decourty L, Joly N, Ricard F, Beggs JD, Legrain P. 2000. Genome-wide protein interaction screens reveal functional networks involving Sm-like proteins. *Yeast 17*:95–110.
Hanley QS, Subramaniam V, Arndt-Jovin DJ, Jovin TM. 2001. Fluorescence lifetime imaging: Multi-point calibration, minimum resolvable differences, and artifact suppression. *Cytometry 43*:248–260.
Hentze MW, Kulozik AE. 1999. A perfect message: RNA surveillance and nonsense-mediated decay. *Cell 96*:307–310.
Hermann H, Fabrizio P, Raker VA, Foulaki K, Hornig H, Brahms H, Lührmann R. 1995. snRNP Sm proteins share two evolutionarily conserved sequence motifs which are involved in Sm protein–protein interactions. *EMBO J 14*:2076–2088.
Kambach C, Walke S, Young R, Avis JM, de la Fortelle E, Raker VA, Lührmann R, Li J, Nagai K. 1999. Crystal structures of two Sm protein complexes and their implications for the assembly of the spliceosomal snRNPs. *Cell 96*:375–387.
Liu Q, Fischer U, Wang F, Dreyfuss G. 1997. The spinal muscular atrophy disease gene product, SMN, and its associated protein SIP1 are in a complex with spliceosomal snRNP proteins. *Cell 90*:1013–1021.
Lykke-Andersen J. 2002. Identification of a human decapping complex associated with hUpf proteins in nonsense-mediated decay. *Mol Cell Biol 22*:8114–8121.
Mayes AE, Verdone L, Legrain P, Beggs JD. 1999. Characterization of Sm-like proteins in yeast and their association with U6 snRNA. *EMBO J 18*:4321–4331.
Mitchell P, Tollervey D. 2000. mRNA stability in eukaryotes. *Curr Opin Genet Dev 10*:193–198.
Miyawaki A, Tsien RY. 2000. Monitoring protein conformations and interactions by fluorescence resonance energy transfer between mutants of green fluorescent protein. *Methods Enzymol 327*:472–500.
Mura C, Cascio D, Sawaya MR, Eisenberg DS. 2001. The crystal structure of a heptameric archaeal Sm protein: Implications for the eukaryotic snRNP core. *Proc Natl Acad Sci USA 98*:5532–5537.
Pannone BK, Do Kim S, Noe DA, Wolin SL. 2001. Multiple functional interactions between components of the Lsm2-Lsm8 complex, U6 snRNA, and the yeast La protein. *Genetics 158*:187–196.
Pannone BK, Xue D, Wolin SL. 1998. A role for the yeast La protein in U6 snRNP assembly: Evidence that the La protein is a molecular chaperone for RNA polymerase III transcripts. *EMBO J 17*:7442–7453.
Patterson GH, Piston DW, Barisas BG. 2000. Forster distances between green fluorescent protein pairs. *Anal Biochem 284*:438–440.
Pillai RS, Will CL, Lührmann R, Schümperli D, Müller B. 2001. Purified U7 snRNPs lack the Sm proteins D1 and D2 but contain Lsm10, a new 14 kDa Sm D1-like protein. *EMBO J 20*:5470–5479.
Raker VA, Plessel G, Lührmann R. 1996. The snRNP core assembly pathway: Identification of stable core protein heteromeric complexes and an snRNP subcore particle in vitro. *EMBO J 15*:2256–2269.
Salgado-Garrido J, Bragado-Nilsson E, Kandels-Lewis S, Séraphin B. 1999. Sm and Sm-like proteins assemble in two related complexes of deep evolutionary origin. *EMBO J 18*:3451–3462.
Séraphin B. 1995. Sm and Sm-like proteins belong to a large family: Identification of proteins of the U6 as well as the U1, U2, U4 and U5 snRNPs. *EMBO J 14*:2089–2098.
Tharun S, He W, Mayes AE, Lennertz P, Beggs JD, Parker R. 2000. Yeast Sm-like proteins function in mRNA decapping and decay. *Nature 404*:515–518.
Tharun S, Parker R. 2001. Targeting an mRNA for decapping: Displacement of translation factors and association of the Lsm1p-7p complex on deadenylated yeast mRNAs. *Mol Cell 8*:1075–1083.
Tomasevic N, Peculis BA. 2002. Xenopus LSm proteins bind U8 snoRNA via an internal evolutionarily conserved octamer sequence. *Mol Cell Biol 22*:4101–4112.
Törö I, Thore S, Mayer C, Basquin J, Séraphin B, Suck D. 2001. RNA binding in an Sm core domain: X-ray structure and functional analysis of an archaeal Sm protein complex. *EMBO J 20*:2293–2303.
Tucker M, Parker R. 2000. Mechanisms and control of mRNA decapping in *Saccharomyces cerevisiae*. *Annu Rev Biochem 69*:571–595.
Vidal VP, Verdone L, Mayes AE, Beggs JD. 1999. Characterization of U6 snRNA–protein interactions. *RNA 5*:1470–1481.
Wang Z, Kiledjian M. 2001. Functional link between the mammalian exosome and mRNA decapping. *Cell 107*:751–762.